

Copolymerization of Vinylidene Fluoride and Hexafluoropropylene in Supercritical Carbon Dioxide

Hongyun Tai, Wenxin Wang, and Steven M. Howdle*

School of Chemistry, University of Nottingham, University Park, Nottingham NG7 2RD, UK

Received June 1, 2005; Revised Manuscript Received August 28, 2005

ABSTRACT: Vinylidene fluoride (VDF) and hexafluoropropylene (HFP) were copolymerized in supercritical carbon dioxide (scCO₂) by a free radical mechanism with and without the use of a fluorinated graft poly(methyl vinyl ether-*alt*-maleic anhydride) copolymer (F-*g*-PMVE-MA) stabilizer. A series of VDF–HFP copolymers, with composition varying from 1.46 to 25.62 mol % (HFP in copolymer), were synthesized with yields in the range 25–54 wt %. The reactivity ratios of VDF and HFP in CO₂ were estimated as $r_{\text{VDF}} = 5.13$ and $r_{\text{HFP}} \approx 0$. The weight-average molecular weights of copolymers, relative to narrow standard poly(methyl methacrylate), were between 35 and 188 kg/mol, and the polydispersity was between 1.4 and 3.1. A solubility study demonstrated that VDF–HFP copolymers were more soluble in CO₂ than in VDF or HFP. In addition, F-*g*-PMVE-MA was found to act as a stabilizer for the copolymerization of VDF and HFP in scCO₂, leading to products with higher molecular weight and improved morphology.

Introduction

Poly(vinylidene fluoride) (PVDF) is a semicrystalline fluoroplastic which possesses excellent thermal, chemical, and weather stability and is used primarily for the applications of pipes, valves, coatings, and films as well as being an acceptable biomaterial.¹ However, crystalline homopolymer fluoroplastics exhibit various drawbacks, including costly processing and having poor solubility in classical organic solvents which can hinder characterization and limits some of their applications as films and coatings where solvents are necessary.² One of the solutions to avoid these drawbacks is copolymerization.² Hexafluoropropylene (HFP) is a common commercial comonomer for VDF. VDF–HFP copolymers have a variety of applications, e.g., Solex fluoroplastic (Solvay Solexis) with a low HFP content (5 mol %) and amorphous fluoroelastomers with high HFP content (20 mol %) (Viton (DuPont), Tecnoflon (Solvay Solexis), and Fluorel (3M/Dynon)). Thermoplastic VDF–HFP copolymer is used for cables and wires because of its flexibility; VDF–HFP fluoroelastomers are used for sealing applications for hostile environments in aircraft, aerospace, automotive, chemical, petroleum, and energy industries.³ Conventional methods for the preparation of PVDF homo- and copolymers are via aqueous suspension or emulsion polymerizations. There are many investigations of free radical (co)-polymerization of VDF by aqueous emulsion and suspension techniques.^{2,4–7} Both generate a large quantity of wastewater and require a substantial quantity of energy to dry the polymer product.³

CO₂ is inexpensive, nontoxic, and nonflammable and readily available in high purity from a variety of sources. Supercritical carbon dioxide (scCO₂) has generated much interest in the polymer synthesis and polymer materials processing communities as an attractive alternative solvent.⁸ Since CO₂ is an ambient gas, polymers can be isolated from the reaction mixture by

a simple depressurization, resulting in a dry polymer product. This eliminates the necessity for energy-intensive drying procedures often required in polymer manufacture. Recently, continuous precipitation polymerization of VDF in scCO₂ has been reported.^{9–11} Also, the dispersion polymerization of VDF in scCO₂ using a range of VDF-based copolymers as stabilizers has been investigated.¹² However, no distinctive spherical particles were obtained. We have investigated the batch precipitation polymerization of VDF in scCO₂ and reported¹³ that commercially available poly(dimethylsiloxane monomethacrylate) (PDMS-*ma*) has a clear effect on the homopolymerization of VDF in scCO₂, leading to high molecular weight products with a broad molecular weight distribution (MWD) and primary particles (200–500 nm) that coagulate to form larger uniform coarse particles (200–500 μm).¹⁴ We also reported that a fluorinated graft poly(methyl vinyl ether-*alt*-maleic anhydride) (F-*g*-PMVE-MA) was an effective stabilizer for the polymerization of VDF in scCO₂.¹⁵ Shoichet and co-workers have investigated the copolymerization of VDF and vinyl acetate in scCO₂ by a free radical mechanism without the use of a stabilizer.¹⁶ A tacky solid copolymer was obtained and the copolymer contained less than 23 mol % VDF.

Here, we investigate the copolymerization of VDF and HFP in scCO₂ in the absence and presence of F-*g*-PMVE-MA stabilizer by a batch process in a 60 mL autoclave. Copolymers with high purity are required for advanced applications such as coatings and electronic components. A scCO₂ route might well simplify the production procedures by eliminating costly and energy-intensive washing and drying operations that are currently employed.

Experimental Section

Materials. The initiator for the copolymerization of VDF and HFP, diethyl peroxydicarbonate (DEPDC), was synthesized according to published methods.¹⁷ The final product solution was ~10 wt % DEPDC in 1,1,2-trichlorotrifluoroethane (Freon 113) and stored at –15 °C. VDF and HFP monomers were donated by Solvay Research, Belgium, and

* Corresponding author: Tel 0115 951 3486; Fax 0115 951 3058; e-mail Steve.Howdle@nottingham.ac.uk.

Table 1. Reaction Conditions and Properties of Vinylidene Fluoride–Hexafluoropropylene (VDF–HFP) Copolymers Produced in Supercritical Carbon Dioxide in the Absence of Stabilizers^a

entry	[M], ^b kg/L	HFP in feed, mol %	HFP in copolymer, ^c mol %	yield, ^d wt %	polymer appearance	GPC results		DSC results		
						<i>M_w</i> , ^e kg/mol	PDI ^f	<i>T_m</i> , ^g °C	cryst, ^h %	<i>T_g</i> , ⁱ °C
1	0.45	5.67	1.46	54.0	coagulated solid	188	2.3	164.8	42.4	
2	0.42	16.88	3.96	42.5	fine powder	98	1.8	147.8	22.5	
3	0.43	33.17	13.05	30.0	elastic solid	64	1.8	80.3	16.5	−30.5
4	0.41	42.90	17.85	28.6	tacky solid	46	1.4			−27.7
5	0.41	70.00	25.62	25.1	sticky solid	35	1.4			−11.3

^a Copolymerizations were carried out at a temperature of 55 °C, an initial vessel pressure of 4000 psi (27.21 MPa), concentration of initiator [I] 1.5 mmol/L, stirring rate 100 rpm, and reaction time 8 h. ^b Concentration of feed monomers. ^c Determined by ¹⁹F NMR. ^d Defined as the weight percentage of the copolymer obtained with respect to the total amount of feed monomers. ^e Weight-average molecular weight. ^f Polydispersity. ^g Melting point. ^h Degree of crystallinity determined by DSC. ⁱ Glass transition temperature.

used without further purification. Carbon dioxide (SFC grade) was purchased from BOC and used without further purification. The fluorinated graft stabilizer (F-g-PMVE-MA) was synthesized by a thermal ring-opening esterification using poly(methyl vinyl ether-*alt*-maleic anhydride (PMVE-MA) (number-average molecular weight *M_n* as 79.8 kg/mol, Aldrich Chemical Co.) and 1*H*,1*H*,2*H*,2*H*-perfluorooctan-1-ol (PFOL) (purity 97%, Lancaster Synthesis) according to the published method.¹⁵

Copolymerization Procedures. Copolymerizations were carried out in a 60 mL stainless steel autoclave¹⁴ at 55 °C, with stirring at 100 rpm, an initial vessel pressure of 4000 psi (27.21 MPa), the total monomer weight of 25 g (i.e., concentration [M] 0.4 kg/L), and concentration of initiator [I] 1.5 mmol/L. Copolymerizations were stopped after 8 h by cooling the reactor to room temperature. Stirring was stopped, and the reactor was slowly vented and opened. The copolymers were obtained as white coagulated solids, or fine powders, or tacky solids depends on the composition of the copolymers. The copolymer products were collected from the autoclave and weighed (*W*₁). Any copolymer products left on the wall and stirrer of the autoclave were washed out by dissolving in THF, precipitated in hexane, and then collected and dried (*W*₂). The yield of each reaction was defined as the weight percentage of the copolymers (*W*₁ + *W*₂) with respect to the total amount of feed monomers. The concentration of stabilizer [S] was 0.52 wt % (weight/weight relative to feed monomers) where needed.

Characterization. Gel permeation chromatography (GPC) was performed at 80 °C using a K-501 HPLC pump with two PLgel 5 μm MIXED-C columns (300 × 7.5 mm, particle size 5 μm, with its linear calibration range of *M_w* 200–2 000 000 g/mol), 1 PLgel 5 μm guard column (50 × 7.5 mm, particle size 5 μm), and refractive index detector. *N,N*-Dimethylformamide (DMF) modified with 0.1 M LiBr was used as the solvent. DMF is a polar solvent and PVDF is a polar polymer. Therefore, there is a dipole interaction, causing artificial shoulders to appear on the high molecular weight end of the distribution. This interaction is eliminated by the addition of LiBr. Moreover, the molecular weight data collected by this GPC measurement are relative to the narrow molecular weight distribution standards of poly(methyl methacrylate) (PMMA) (Polymer Laboratories Ltd.). The calibration curve of PMMA was obtained at 80 °C.

¹H and ¹⁹F NMR spectra for VDF–HFP copolymers were obtained in DMF-*d*₇ using a Bruker 300 MHz spectrometer, using tetramethylsilane (TMS) or CFCl₃ as internal reference of ¹H and ¹⁹F NMR spectroscopy, respectively. The morphology of VDF–HFP copolymers was determined using a Philips XL30 SEM machine. DSC analysis of copolymers was performed using TA Instrument MDSC 2920 following standard procedures (ASTM D3418-99). Samples were heated to 220 °C at a rate of 10 °C/min from room temperature and then cooled to −50 °C at the same rate. After 5 min isothermal process, samples were heated to 220 °C at 10 °C/min again (second heating cycle) and the data collected. The melting temperature (*T_m*), glass transition temperature (*T_g*), and crystallinity of the copolymers were determined by the second heating curves.

Solubility Test. The solubility of the copolymers in pure scCO₂ as well as in pure VDF, pure HFP, and a mixture of

assignments	¹⁹ F δ (ppm) vs CFCl ₃	integrals
–CH ₂ CF ₂ CH ₂ CF ₂ –	–93, –94 to –96	S _A
CH ₂ CF ₂ CF ₂ CF(CF ₃)–	–109 and –111	
–CH ₂ CF ₂ CF ₂ CH ₂ –	–113 and –117	
–CF ₂ CF(CF ₃)–	–71 and –76	S _B
–CF ₂ CF(CF ₃)–	–118 and –119	
–CF ₂ CF(CF ₃)–	–182	

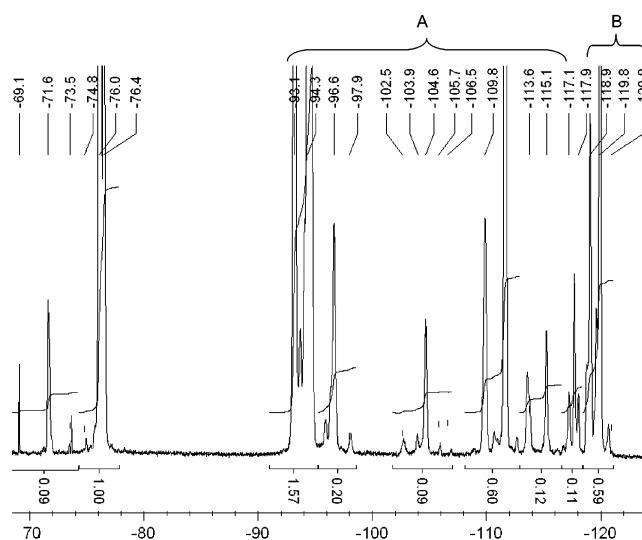


Figure 1. ¹⁹F NMR spectrum for the VDF–HFP copolymer and the peak assignments. Note that the compositions of VDF–HFP copolymers were determined by the integrals of characteristic peaks A and B.

VDF/HFP/CO₂ was studied using a hydraulic variable volume view cell¹⁸ equipped with a sapphire window and a moving piston fabricated completely from sapphire. The cell volume is variable from 13 to 43 mL and can be accurately controlled. The maximum pressure for the view cell is 6000 psi (40.82 MPa). The copolymer (0.26 g) was placed in the view cell, which was then sealed. CO₂, VDF, or HFP (21 g) was transferred into the cell through a sample vessel cylinder (80 mL, maximum pressure 1800 psi (12.24 MPa)). The cell was heated to the desired temperature, and then the pressure was increased by decreasing the volume of the cell to observe the solubility of the copolymer.

Results and Discussion

A range of copolymers were successfully synthesized in scCO₂ and characterized for their composition, molecular weight, molecular weight distribution, *T_m*, and *T_g* (Table 1).

Compositions of VDF–HFP Copolymers. The copolymer composition was controlled by the monomer feed concentration (5.67–70 mol % HFP) and determined by ¹⁹F NMR (Figure 1). The ¹⁹F NMR spectrum exhibits various groups of signals,¹⁹ those assigned to VDF units are centered at −93, −94 to −96 ppm for

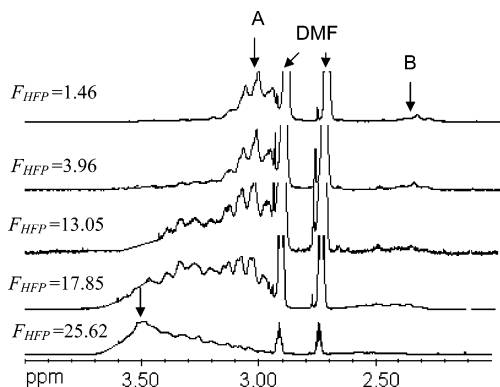


Figure 2. ^1H NMR spectra for VDF-HFP copolymers. Note that the multiplet signal for head-to-tail normal addition groups ($-\text{CH}_2-\text{CF}_2-\text{CH}_2-\text{CF}_2-$, A) shows a low field shift from 3.1 to 3.5 ppm, and the multiplet signal at 2.35 ppm for tail-to-tail reversed addition groups ($-\text{CF}_2-\text{CH}_2-\text{CH}_2-\text{CF}_2-$, B) decreases while increasing HFP mole fraction in the copolymers.

head-to-tail normal additions ($-\text{CH}_2\text{CF}_2\text{CH}_2\text{CF}_2-$), at -109 and -111 ppm for difluoromethylene groups adjacent to a HFP base unit ($\text{CH}_2\text{CF}_2\text{CF}_2\text{CF}(\text{CF}_3)-$), at -113 and -117 ppm for the head-to-head reversed addition ($-\text{CH}_2\text{CF}_2\text{CF}_2\text{CH}_2-$), and at -104 ppm for CF_2 group adjacent to initiator radical end groups. Those assigned to HFP units signals are centered at -71 and -76 ppm for the pendant CF_3 group ($-\text{CF}_2\text{CF}(\text{CF}_3)-$), at -118 and -119 ppm for CF_2 ($-\text{CF}_2\text{CF}(\text{CF}_3)-$) group, and at -182 ppm for the CF ($-\text{CF}_2\text{CF}(\text{CF}_3)-$) group.

According to the integrals of the characteristic peaks of VDF and HFP, it was possible to assess the mol % of HFP monomer in the copolymer (F_{HFP}) as eq 1.

$$F_{\text{HFP}} = \frac{S_B}{S_A + S_B} \quad (1)$$

where S_A and S_B represent the integral of the signals A and B in the ^{19}F NMR spectrum (Figure 1). In all cases, the molar percentage of VDF in the copolymer is higher than that in the feed, indicating that VDF has higher reactivity than HFP in scCO_2 .

The ^1H NMR spectra (Figure 2) exhibit the presence of both signals centered at 3.10 (A) and 2.35 (B) ppm, assigned to the methylene groups of PVDF units in the copolymers (those of head-to-tail normal addition ($-\text{CH}_2-\text{CF}_2-\text{CH}_2-\text{CF}_2-$) and tail-to-tail reversed addition ($-\text{CF}_2-\text{CH}_2-\text{CH}_2-\text{CF}_2-$), respectively).¹⁹ The multiplet signal for head-to-tail normal addition groups shows a low field shift from 3.1 to 3.5 ppm, and the multiplet signal at 2.35 ppm for tail-to-tail reversed addition groups decreases while increasing HFP mole fraction in the copolymers.

Reactivity Ratios for VDF-HFP Copolymerizations in scCO_2 . Fluorinated monomers are less reactive toward electrophilic radicals compared to their hydrogenated homologues; on the other hand, they are generally more reactive toward nucleophilic radicals.^{20,21} It is reported that reactivity ratios for copolymerization of VDF with HFP in solution or emulsion polymerizations are $r_{\text{VDF}} = 6.7/r_{\text{HFP}} \approx 0.22$ or $r_{\text{VDF}} = 2.45/r_{\text{HFP}} \approx 0.23$. Reactivity ratios are the result of a combination of steric, resonance, and polar effects²⁴ and indicate that HFP is less reactive than VDF and cannot undergo self-propagation; i.e., HFP cannot homopolymerize in solution or emulsion. Using only HFP monomer in scCO_2

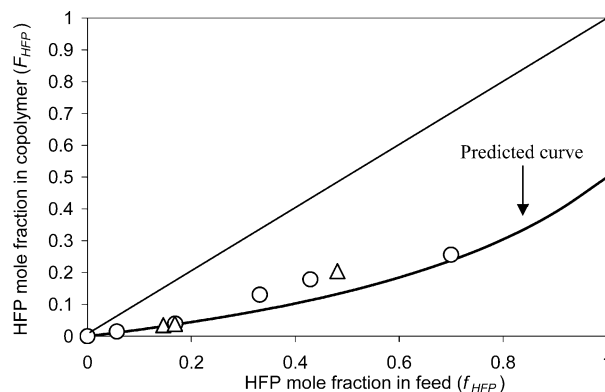


Figure 3. Dependence of the copolymer composition (F_{HFP}) on the composition of feed monomers (f_{HFP}): O, obtained in the absence of stabilizers (Table 1); Δ, obtained in the presence of F-g-PMVE-MA (Table 2). Note that the experimental data are fitted well with the predicted curve, based on estimated reactivity ratios $r_{\text{VDF}} = 5.13$ and $r_{\text{HFP}} \approx 0$.

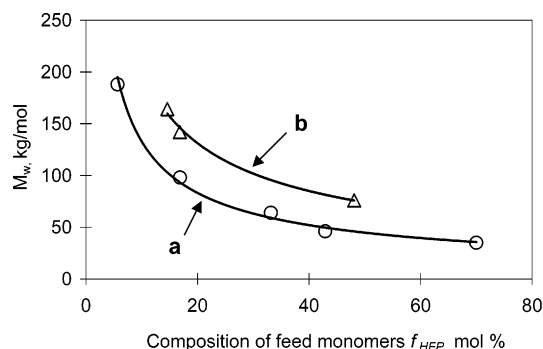


Figure 4. Relationship of the composition of feed monomers (f_{HFP}) and weight-average molecular weight (M_w): O, obtained in the absence of stabilizers (Table 1); Δ, obtained in the presence of F-g-PMVE-MA (Table 2). Note that M_w of the copolymers was found to decrease with increasing HFP concentration in the feed. Clearly, these are consequences of the low reactivity of HFP and the decrease of VDF concentration. The trend curve b is well above the trend curve a, indicating higher M_w copolymer products were obtained in the presence of stabilizers.

under the same reaction conditions as stated in Table 1, we demonstrated that even after 8 h HFP did not homopolymerize. Therefore, the reactivity ratio of HFP in scCO_2 approaches zero, as reported in the literature for other reaction media. Therefore, in the copolymerization of VDF and HFP in scCO_2 , HFP only underwent cross-propagation with VDF, but VDF self-propagates randomly and also cross-propagates with HFP.

In all experiments (Table 1), the total monomer concentration in the autoclave was kept constant as ca. 0.4 kg/L. As the comonomer mixtures prepared became more HFP-rich, the overall polymerization rate decreased. Therefore, the yield and molar mass of VDF-HFP copolymers decreased with increasing HFP in the feed (entries 1–5 in Table 1).

The reactivity ratios can be estimated using the differential form of the Mayo-Lewis equation, i.e., copolymer composition equation, as described in eq 2.²⁵

$$F_{\text{HFP}} = \frac{r_{\text{HFP}}f_{\text{HFP}}^2 + f_{\text{HFP}}(1 - f_{\text{HFP}})}{r_{\text{HFP}}f_{\text{HFP}}^2 + 2f_{\text{HFP}}(1 - f_{\text{HFP}}) + r_{\text{VDF}}(1 - f_{\text{HFP}})^2} \quad (2)$$

The terms F_{HFP} and f_{HFP} represent the instantaneous

Table 2. Reaction Conditions and Properties of Vinylidene Fluoride–Hexafluoropropylene (VDF–HFP) Copolymers Produced in Supercritical Carbon Dioxide in the Presence of the Fluorinated Graft Poly(methyl vinyl ether-*alt*-maleic anhydride) (F-*g*-PMVE-MA) Stabilizer^a

entry	[M], ^b kg/L	[S], ^j wt %	HFP in feed, mol %	HFP in copolymer, ^c mol %	yield, ^d wt %	polymer appearance	GPC results		DSC results		
							M_w , ^e kg/mol	PDI ^f	T_m , ^g °C	cryst, ^h %	T_g , ⁱ °C
1	0.43	1.96	14.60	3.46	44.0	fine powder	164	2.8	145.2	27.6	
2	0.42	4.96	16.83	3.90	37.9	fine powder	142	3.1	147.6	24.3	
3	0.41	2.01	48.10	20.45	30.5	tacky solid	76	1.9			−20.5

^{a–i} See notes in Table 1. ^j Weight percentage of stabilizer with respect to the total amount of feed monomers.

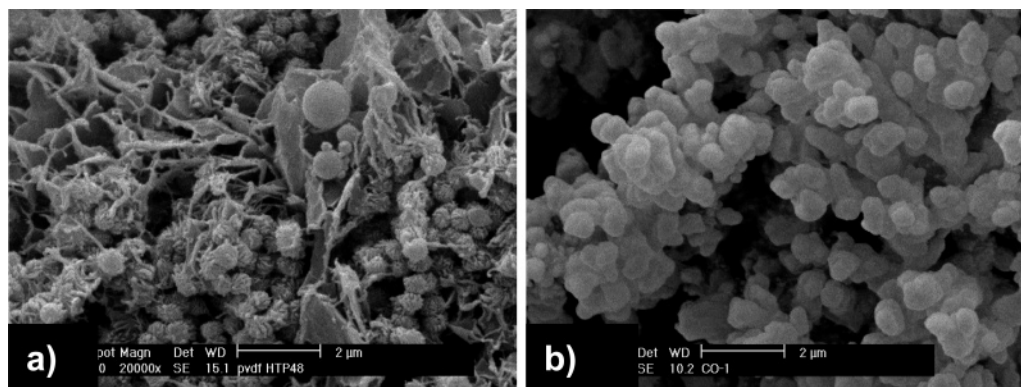


Figure 5. SEM images for VDF–HFP copolymers (b) produced in scCO_2 , in comparison with VDF homopolymer (a) produced under the same conditions. Note that the morphology of the copolymer demonstrated agglomerated particles (b) rather than a porous structure (a) for the homopolymer.

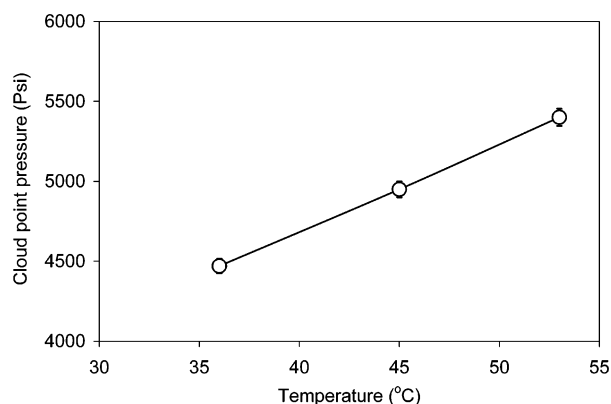


Figure 6. Cloud point curve for VDF–HFP copolymer B ($F_{\text{HFP}} = 25.62$, 1.11 wt %) in CO_2 . Errors are within 1%.

mole fraction of HFP in the copolymer and in the feed, respectively. Because $r_{\text{HFP}} \approx 0$, eq 2 can be simplified as eq 3.

$$\frac{1}{F_{\text{HFP}}} = \frac{r_{\text{VDF}}}{f_{\text{HFP}}} - r_{\text{VDF}} + 2 \quad (3)$$

To estimate reactivity ratios, one has to assume that the concentrations of two macroradicals (VDF and HFP) remain constant (steady-state treatment) and to neglect compositional drift. This requires the monomer conversion to be controlled at a low level (less than 5%).²⁴ The experimental data in Table 1 do not satisfy this assumption. To obtain the values of reactivity ratio, two experiments were carried out at a low monomer conversion (<5%); the mole percentages of HFP in the copolymer and the feed (F_{HFP} , f_{HFP}) obtained were (5.3, 22.80) and (21.80, 50.50), respectively. Applying these data into eq 3 resulted in a value of r_{VDF} of 5.13 ± 0.44 . These

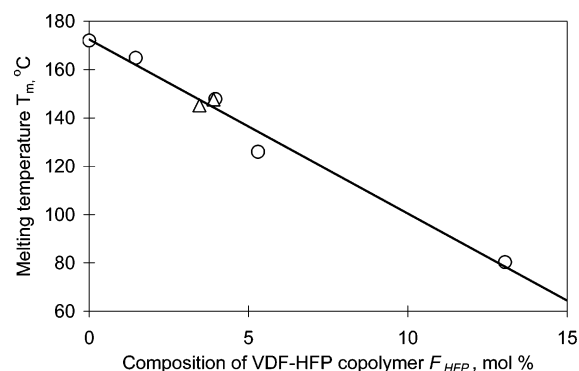


Figure 7. Dependence of the melting temperature (T_m) on the copolymer composition (F_{HFP}): \circ , obtained in the absence of stabilizers (Table 1); \triangle , obtained in the presence of F-*g*-PMVE-MA (Table 2). Note that melting peaks linearly decrease with the increase of HFP content.

experimental results show that the reactivity ratios for VDF and HFP in scCO_2 are fairly close to the literature data for conventional solution and emulsion copolymerizations of VDF and HFP. Figure 3 summarizes the experimental F_{HFP} vs f_{HFP} data (cf. Tables 1 and 2), which fit well with the predicted curve based on estimated reactivity ratios, $r_{\text{VDF}} = 5.13$ and $r_{\text{HFP}} \approx 0$.

Molecular Weight and Molecular Weight Distribution of VDF–HFP Copolymers. The molecular weight of the copolymers was found to decrease with increasing HFP concentration in the feed (Table 1 and Figure 4), while the molecular weight distribution became increasingly narrow. Clearly, these are consequences of the lower overall propagation rate due to the addition of HFP and the decrease of VDF concentration.

Morphologies of VDF–HFP Copolymers. The VDF–HFP copolymers were obtained as coagulated solids through to viscous solids with increasing HFP

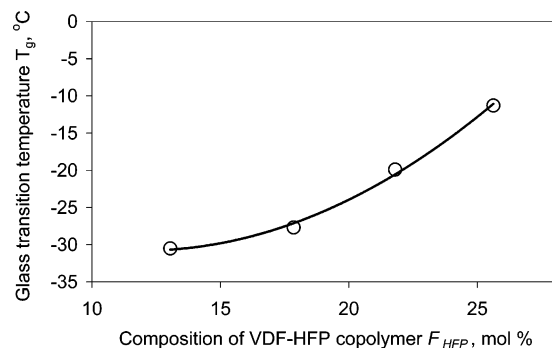


Figure 8. Dependence of the glass transition temperature (T_g) on copolymer composition. Note that T_g increases with increasing HFP content because the introduction of HFP units lowers the conformational flexibility.

contents (Table 1). At HFP content of 16.88 mol % in the feed monomers, the product copolymer was a white fine powder (entry 2 in Table 1). The morphology displayed by SEM analysis (b in Figure 5) showed aggregated particles, completely different from the porous material (a in Figure 5) for PVDF homopolymer produced under the same conditions in $scCO_2$. These results indicate that the addition of HFP led to the formation of copolymer particles. Both the solvency conferred by the presence of HFP and the subsequent decrease of crystallinity in the copolymers are important factors in this change of morphology.

Solubility of VDF-HFP Copolymers in CO_2 . PVDF is a semicrystalline polymer with high crystallinity (greater than 50%) and is insoluble in most organic solvents at room temperature, with the exception of highly polar solvents such as DMF. By contrast, VDF-HFP copolymers are soluble in THF at room temperature. It has been reported that VDF-HFP copolymers are more soluble in $scCO_2$ than PVDF because the VDF-HFP copolymer has a larger free volume.²⁶

Using the view cell apparatus, we have investigated the solubility of VDF-HFP copolymer A ($F_{HFP} = 17.85$, entry 4 in Table 1) in $scCO_2$ at a concentration of 1.02 wt %. We found that it was not totally soluble over a range of accessible conditions, from 35 to 65 °C at all pressures up to the maximum safe working pressure of 6000 psi (40.82 MPa). However, it was clear that there was some partial solubility because a cloudy transition point was observed when the pressure of the cell was lowered from 6000 psi (40.82 MPa). By contrast, for copolymer B ($F_{HFP} = 25.62$, entry 5 in Table 1), which one might expect to be more soluble, at 1.11 wt % this was found to totally dissolve in pure $scCO_2$ but only at pressures that were significantly higher than those that could be used safely for carrying out the copolymerization reaction, i.e., above 4500 psi (30.61 MPa) (Figure 6).

This more soluble material, copolymer B, was also tested in pure VDF and pure HFP at the same concentrations and was found to be not totally soluble in either VDF or HFP at the highest accessible pressure 6000 psi (40.82 MPa) between 35 and 65 °C. Therefore, CO_2 is a better solvent for the VDF-HFP copolymer than its monomers, VDF and HFP. In addition, we have investigated the solubility of the more soluble copolymer B in a mixture of CO_2 , VDF, and HFP to mimic the reaction conditions. At two different loadings of copolymer B (1 and 20 wt %), we found that the copolymer

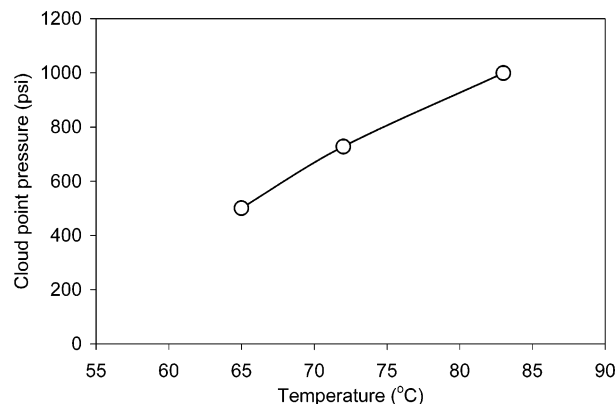


Figure 9. Cloud point curve for F-g-PMVE-MA (1.2 wt %) in HFP. Note that F-g-PMVE-MA was found to be soluble in liquid HFP below 65 °C.

could not form a homogeneous solution in such a mixture. The particular mixture chosen (30 wt % of monomers in the ternary mixture and 70 mol % of HFP in the monomers) was tested over a range of conditions, including those that correspond to our reaction conditions (55 °C and 4000 psi). Theoretically, the solubility of the copolymer in CO_2 increases with the HFP content in the copolymer. Copolymer B has the highest HFP content among the copolymers synthesized in this work and is therefore the most soluble. Since this copolymer is not soluble in the mixture of CO_2 , VDF, and HFP, then none of the copolymers synthesized are likely to be soluble. Moreover, as the copolymerization proceeds, the composition of monomers in the mixture changes due to the different reactivity ratios of the monomers. VDF has a high reactivity ratio while HFP does not homopolymerize at the reaction conditions,^{23,27,28} and this will lead to the composition drift in the copolymer; i.e., the HFP composition in the copolymer will increase with the conversion. Therefore, compared to the overall final average composition, a copolymer with a lower HFP content is formed in the early polymerization stage, and this material will likely have a lower solubility than the final product.

Thermal Properties of VDF-HFP Copolymers.

A series of experiments were carried out at different feed compositions to investigate the influence of the copolymer composition on thermal properties (melting temperature (T_m) and glass transition temperature (T_g)) (Table 1) while keeping the other conditions constant. Melting peaks (entries 1–3 in Table 1) linearly decrease with the increase of HFP content (Figure 7). However, no melting peaks were observed for copolymers with high HFP mole percentages (entries 4 and 5 in Table 1).

The degree of crystallinity for copolymers was determined from the melting enthalpy by DSC. The standard heat of fusion used for calculation is 104.5 J/g,²⁹ the melting enthalpy (ΔH_0) of totally crystalline PVDF polymer. As one would expect, the degree of crystallinity for VDF-HFP copolymers (Table 1) was much lower than PVDF homopolymer (>50%) and decreased dramatically with increase of HFP content in the copolymer (entry 3 in Table 1).

Low-temperature flexibility is governed by the glass transition temperature (T_g) which depends mainly on the conformational flexibility of individual chain elements. Therefore, if the various conformational states can be interconverted more freely, T_g is lower and low-

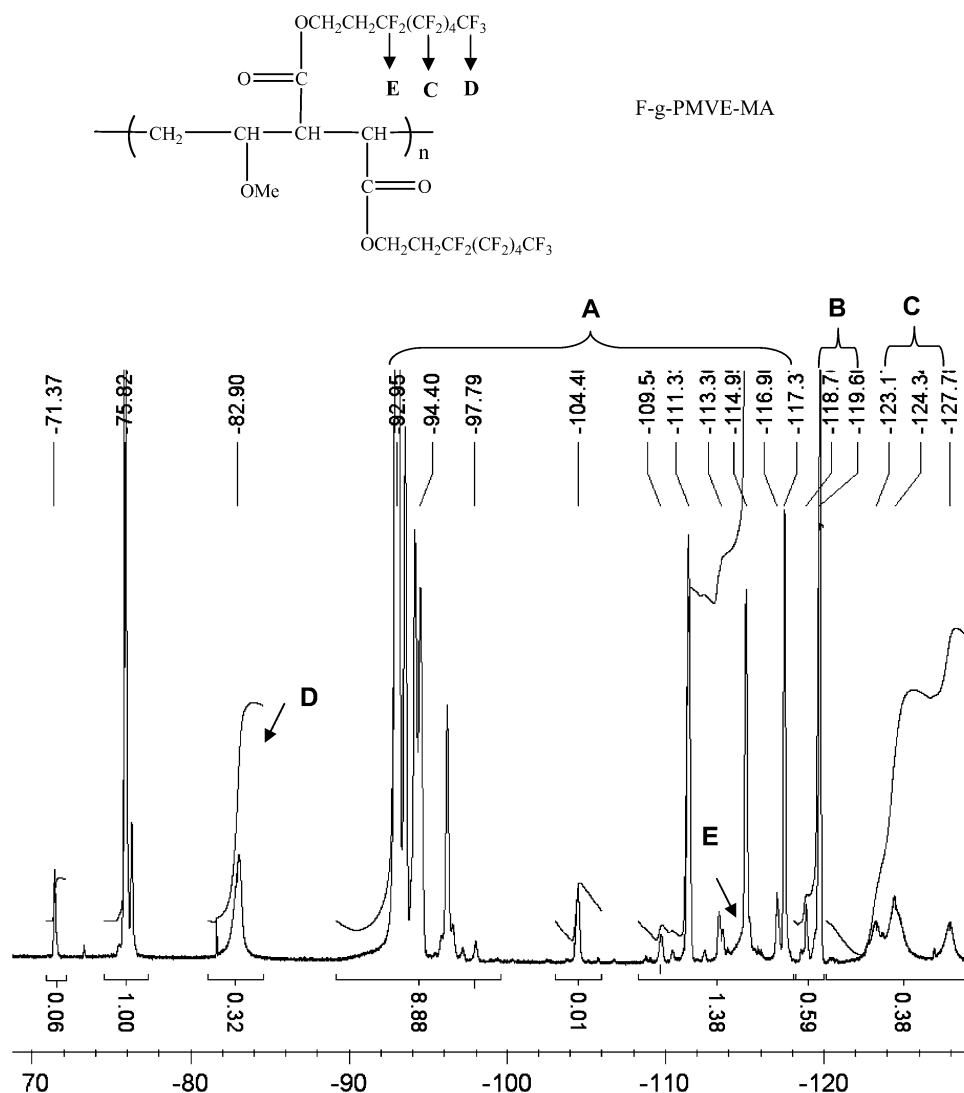


Figure 10. ¹⁹F NMR spectrum of VDF-HFP copolymer synthesized in the presence of F-g-PMVE-MA. Note the assignments for VDF-HFP (A and B); see Figure 1.

temperature performance is better. Thus, a lack of crystallinity and a low T_g value are required for a serviceable elastomer. PVDF has sufficiently low T_g (-40°C), but very strong intermolecular forces cause crystallization and thus restrict conformational freedom. Copolymerization with HFP lowers the crystallinity of PVDF and takes advantages of its low T_g to give a fluoroelastomer with T_g at ca. -20°C .³⁰ Experimental data in Table 1 and Figure 8 demonstrate that the T_g increases with increasing HFP content because the introduction of HFP units lowers the conformational flexibility. A very similar effect has been observed for the copolymerization of 2,2-bis(trifluoromethyl)-4,5-difluoro-1,3-dioxole (PDD) with tetrafluoroethylene (TFE) in scCO_2 .³¹

Impact of the Addition of the Fluorinated Graft Stabilizer. The solubility of PDMS-ma and F-g-PMVE-MA in the comonomer HFP was tested using the variable volume view cell. The results demonstrate that PDMS-ma (1 wt %) was not soluble in HFP at 55°C (the reaction temperature) even when the pressure reached 6000 psi (40.82 MPa). However, F-g-PMVE-MA was found to be soluble in liquid HFP at 55°C , and its cloud point curve above 55°C was collected (Figure 9).

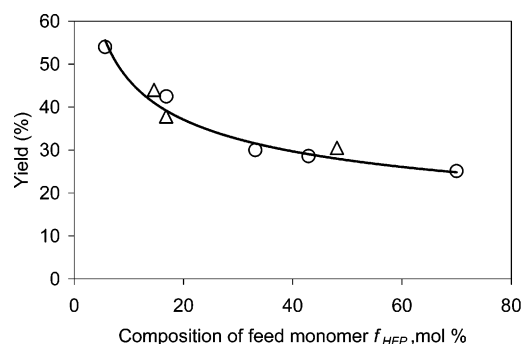


Figure 11. Effect of the HFP content in feed monomers (f_{HFP}) on yields. Note that the yield data for copolymerizations of VDF-HFP in the presence of F-g-PMVE-MA (Δ) showed the same trend as those for copolymerizations without F-g-PMVE-MA present (O).

F-g-PMVE-MA was tested as the stabilizer in the copolymerization of VDF and HFP. Two typical feed monomer compositions were used to synthesize a fluoroelastomer ($f_{\text{HFP}} = 4 \text{ mol } \%$) and a fluoroelastomer ($f_{\text{HFP}} = 20 \text{ mol } \%$) (Table 2).

The ¹⁹F NMR spectrum (Figure 10) for the VDF-HFP copolymer synthesized in the presence of F-g-PMVE-

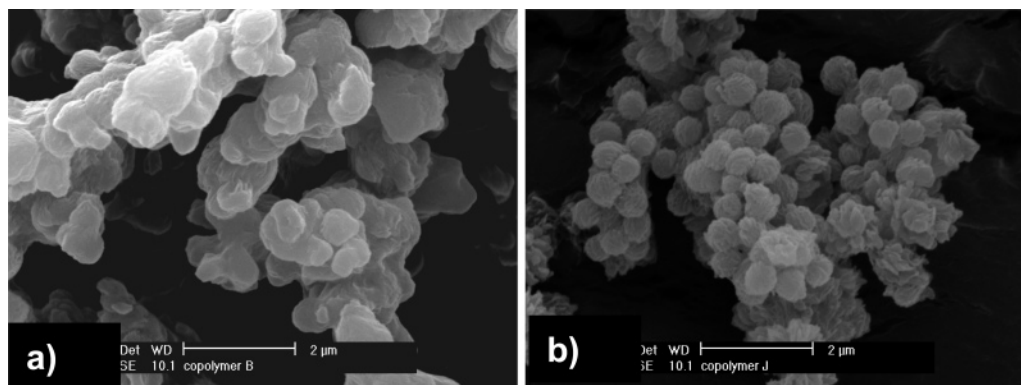


Figure 12. Effect of F-*g*-PMVE-MA on the morphology of VDF-HFP copolymers produced in scCO_2 . Note that more discrete copolymer particles (b) were produced in the presence of 4.96 wt % of F-*g*-PMVE-MA, compared to the coagulated particles (a) produced in the absence of stabilizers.

MA showed the characteristic signals of F-*g*-PMVE-MA at -83 ppm (D), -120 to -130 ppm range (C), and -115 ppm (E).

After purification by purging the copolymer with CO_2 at 55°C for 24 h, the characteristic signals for F-*g*-PMVE-MA disappeared, thus demonstrating very little incorporation of the stabilizer into the copolymers. The copolymer composition was also calculated using eq 1.

The yield data for copolymerizations of VDF-HFP in the presence of F-*g*-PMVE-MA showed the same trend as those for copolymerizations without F-*g*-PMVE-MA present (Figure 11). These data indicate that the addition of F-*g*-PMVE-MA does not have strong impact on yield, the same as the observations for the homopolymerization of VDF in scCO_2 .¹⁵

At low HFP feed (ca. 15 mol %), the molecular weight of the copolymer increased dramatically in the presence of F-*g*-PMVE-MA (cf. entry 2 in Table 1 and entry 1 in Table 2). The morphology was also improved slightly. At high stabilizer loadings (4.96 wt %, entry 2 in Table 2), the morphology showed some spherical particles (b in Figure 12).

At high HFP feed (48 mol %), the molecular weight of the copolymer also increased significantly in the presence of F-*g*-PMVE-MA stabilizer (cf. entry 4 in Table 1 and entry 3 in Table 2). The curve of M_w vs F_{HFP} for the copolymer products synthesized in the presence of stabilizers (b in Figure 4) is well above the one for the products synthesized in the absence of stabilizers (a in Figure 4), further indicating the presence of stabilizers leads to higher M_w copolymer products. These results demonstrate that F-*g*-PMVE-MA acts as a stabilizer for the copolymerization of VDF and HFP in scCO_2 . Moreover, DSC and TGA analysis demonstrated that the addition of stabilizer did not unduly influence T_m and T_g of the copolymers (Table 2).

Conclusions

A series of VDF-HFP copolymers, with composition between 1.46 and 25.62 wt % (HFP content), were synthesized in scCO_2 with yields at 25–54 wt %. The weight-average molecular weight of the copolymers, relative to narrow standard poly(methyl methacrylate), were between 35 and 188 kg/mol, and the polydispersity was between 1.6 and 3.0. Moreover, it was found that use of a fluorinated material F-*g*-PMVE-MA led to a stabilized copolymerization of VDF and HFP in scCO_2 and to the products with much higher molecular weight and improved morphology.

Acknowledgment. We gratefully acknowledge the European Community for funding (ECOPOL Project GRD1-2001-40294). We thank also Dr. C. J. Duxbury and Mr. A. Naylor for their advice and Mr. R. G. M. Wilson, Mr. P. A. Fields, and Mr. M. P. Dellar for their technical support. S.M.H. is a Royal Society Wolfson Research Merit Award holder.

References and Notes

- (1) Klinge, U.; Klosterhalfen, B.; Ottinger, A. P.; Junge, K.; Schumpelick, V. *Biomaterials* **2002**, *23*, 3487–3493.
- (2) Ameduri, B.; Boutevin, B. *J. Fluorine Chem.* **2000**, *104*, 53–62.
- (3) Howe-Grant, M. *Fluorine Chemistry: A Comprehensive Treatment*; Wiley: New York, 1995.
- (4) Ameduri, B.; Boutevin, B.; Kostov, G. K.; Petrova, P. *Des. Monomers Polym.* **1999**, *2*, 267–285.
- (5) McCarthy, T. F.; Williams, R.; Bitay, J. F.; Zero, K.; Yang, M. S.; Mares, F. *J. Appl. Polym. Sci.* **1998**, *70*, 2211–2225.
- (6) Apostolo, M.; Albano, M.; Storti, G.; Morbidelli, M. *Macromol. Symp.* **2000**, *150*, 65–71.
- (7) Barber, L. A.; Pennwalt Corp., USA: EP169328, 1986; p 27.
- (8) Woods, H. M.; Silva, M. M. C. G.; Nouvel, C.; Shakesheff, K. M.; Howdle, S. M. *J. Mater. Chem.* **2004**, *14*, 1663–1678.
- (9) Charpentier, P. A.; Kennedy, K. A.; DeSimone, J. M.; Roberts, G. W. *Macromolecules* **1999**, *32*, 5973–5975.
- (10) Charpentier, P. A.; DeSimone, J. M.; Roberts, G. W. *Ind. Eng. Chem. Res.* **2000**, *39*, 4588–4596.
- (11) Saraf, M. K.; Gerard, S.; Wojcinski, L. M.; Charpentier, P. A.; DeSimone, J. M.; Roberts, G. W. *Macromolecules* **2002**, *35*, 7976–7985.
- (12) DeSimone, J. M.; Riddick, L. *Proc. NOBChE* **1999**, *26*, 53–61.
- (13) Liu, J.; Tai, H.; Howdle, S. M. *Polymer* **2005**, *46*, 1467–1472.
- (14) Tai, H.; Wang, W.; Martin, R.; Liu, J.; Lester, E.; Licence, P.; Woods, H. M.; Howdle, S. M. *Macromolecules* **2005**, *38*, 355–363.
- (15) Tai, H.; Wang, W.; Howdle, S. M. *Macromolecules* **2005**, *38*, 1542–1545.
- (16) Baradie, B.; Shoichet, M. S. *Macromolecules* **2002**, *35*, 3569–3575.
- (17) Strain, F.; Bissinger, W. E.; Dial, W. R.; Rudolf, H.; DeWitt, B. J.; Stevens, H. C.; Langston, J. H. *J. Am. Chem. Soc.* **1950**, *72*, 1254–1263.
- (18) Licence, P.; Dellar, M. P.; Wilson, R. G. M.; Fields, P. A.; Litchfield, D.; Woods, H. M.; Poliakoff, M.; Howdle, S. M. *Rev. Sci. Instrum.* **2004**, *75*, 3233–3236.
- (19) Gelin, M. P.; Ameduri, B. *J. Fluorine Chem.* **2003**, *119*, 53–58.
- (20) Giannetti, E. *Polym. Int.* **2001**, *50*, 10–26.
- (21) Dolbier, W. R. *Chem. Rev.* **1996**, *96*, 1557–1584.
- (22) Moggi, G.; Bonardelli, P.; Russo, S. *Conference Conv. Ital. Sci. Macromol.* **1983**, *2*, 405.
- (23) Bonardelli, P.; Moggi, G.; Turturro, A. *Polymer* **1986**, *27*, 905–909.

- (24) Stevens, M. P. *Polymer Chemistry: An Introduction*, 3rd ed.; Oxford University Press: New York, 1999.
- (25) Polic, A. L.; Duever, T. A.; Penlidis, A. *J. Polym. Sci., Polym. Chem.* **1998**, *36*, 813–822.
- (26) Dinoia, T. P.; Conway, S. E.; Lim, J. S.; McHugh, M. A. *J. Polym. Sci., Part B: Polym. Phys.* **2000**, *38*, 2832–2840.
- (27) Apostolo, M.; Arcella, V.; Storti, G.; Morbidelli, M. *Macromolecules* **1999**, *32*, 989–1003.
- (28) Logothetis, A. L. *Prog. Polym. Sci.* **1989**, *14*, 251–296.
- (29) Teyssedre, G.; Bernes, A.; Lacabanne, C. *J. Polym. Sci., Part B: Polym. Phys.* **1993**, *31*, 2027–2034.
- (30) Banks, R. E.; Smart, B. E.; Tatlow, J. C. *Organofluorine Chemistry: Principles and Commercial Applications*; Plenum: New York, 1994.
- (31) Wood, C. D.; Michel, U.; Rolland, J. P.; DeSimone, J. A. *J. Fluorine Chem.* **2004**, *125*, 1671–1676.

MA0511346